AFRL-RX-WP-TP-2014-0013

BEAMING CIRCULARLY POLARIZED PHOTONS FROM QUANTUM DOTS COUPLED WITH PLASMONIC SPIRAL ANTENNA (POSTPRINT)

Robert L. Nelson
AFRL/RXAS

JANUARY 2014
Interim Report

STINFO COPY

AIR FORCE RESEARCH LABORATORY
MATERIALS AND MANUFACTURING DIRECTORATE
WRIGHT-PATTERSON AIR FORCE BASE, OH 45433-7750
AIR FORCE MATERIEL COMMAND
UNITED STATES AIR FORCE

NOTICE AND SIGNATURE PAGE

AFRL-RX-WP-TP-2014-0013 HAS BEEN REVIEWED AND IS APPROVED FOR PUBLICATION IN ACCORDANCE WITH ASSIGNED DISTRIBUTION STATEMENT.

_____//SIGNED//_____
KATIE E. THORP, Program Mgr & Chief
Soft Matter Materials Branch
Functional Materials Division

_____//SIGNED//_____
KAREN R. OLSON, Deputy Chief
Functional Materials Division
Materials & Manufacturing Directorate

REPORT DOCUMENTATION PAGE

Form Approved
OMB No. 0704-0188

1. REPORT DATE *(DD-MM-YY)*	2. REPORT TYPE	3. DATES COVERED *(From - To)*
January 2014	Interim	5 November 2009 – 21 June 2012

4. TITLE AND SUBTITLE
BEAMING CIRCULARLY POLARIZED PHOTONS FROM QUANTUM DOTS COUPLED WITH PLASMONIC SPIRAL ANTENNA (POSTPRINT)

5a. CONTRACT NUMBER
In-House

5b. GRANT NUMBER

5c. PROGRAM ELEMENT NUMBER
62102F

6. AUTHOR(S)
Guanghao Rui - University of Science and Technology of China
Wiebin Chen and Qiwen Zhan - University of Dayton
Don C. Abeysinghe - University of Cincinnati
Robert L. Nelson - AFRL/RXAP

5d. PROJECT NUMBER
4347

5e. TASK NUMBER

5f. WORK UNIT NUMBER
X043 (BN103400)

7. PERFORMING ORGANIZATION NAME(S) AND ADDRESS(ES)
AFRL/RXAS
3005 Hobson Way
Wright-Patterson AFB, OH 45433

8. PERFORMING ORGANIZATION REPORT NUMBER

9. SPONSORING/MONITORING AGENCY NAME(S) AND ADDRESS(ES)
Air Force Research Laboratory
Materials and Manufacturing Directorate
Wright-Patterson Air Force Base, OH 45433-7750
Air Force Materiel Command
United States Air Force

10. SPONSORING/MONITORING AGENCY ACRONYM(S)
AFRL/RXAS

11. SPONSORING/MONITORING AGENCY REPORT NUMBER(S)
AFRL-RX-WP-TP-2014-0013

12. DISTRIBUTION/AVAILABILITY STATEMENT
Approved for public release; distribution unlimited.

14. ABSTRACT
Coupling nanoscale emitters via optical antennas enables comprehensive control of photon emission in terms of intensity, directivity and polarization. In this work we report highly directional emission of circularly polarized photons from quantum dots coupled to a spiral optical antenna. The structural chirality of the spiral antenna imprints spin state to the emitted photons. Experimental results reveal that a circular polarization extinction ratio of 10 is obtainable. Furthermore, increasing the number of turns of the spiral gives rise to higher antenna gain and directivity, leading to higher field intensity and narrower angular width of emission pattern in the far field. For a five-turn Archimedes' spiral antenna, field intensity increase up to 70-fold simultaneously with antenna directivity of 11.7 dB has been measured in the experiment. The highly directional circularly polarized photon emission from such optically coupled spiral antenna may find important applications in single molecule sensing, quantum optics information processing and integrated photonic circuits as a nanoscale spin photon source.

15. SUBJECT TERMS
quantum dots, plasmonic spiral antenna, nanoscale, integrated photonic circuits

16. SECURITY CLASSIFICATION OF:

a. REPORT	b. ABSTRACT	c. THIS PAGE	17. LIMITATION OF ABSTRACT:	18. NUMBER OF PAGES	19a. NAME OF RESPONSIBLE PERSON (Monitor)
Unclassified	Unclassified	Unclassified	SAR	13	Katie E. Thorp

19b. TELEPHONE NUMBER *(Include Area Code)*
(937) 255-9159

Standard Form 298 (Rev. 8-98)
Prescribed by ANSI Std. Z39-18

REPORT DOCUMENTATION PAGE (Cont'd)

7. PERFORMING ORGANIZATION NAME(S) AND ADDRESS(ES)

University of Science and Technology of China
Department of Optics and Optical Engineering
Hefei, Anhui 230026, China

University of Dayton
Electro-Optics Program
300 College Park
Dayton, OH 45469

University of Cincinnati
Department of Electrical and Computer Engineering
Cincinnati, OH 45219

AFRL/RXAP
3005 Hobson Way
Wright-Patterson AFB, OH 45433

Beaming circularly polarized photons from quantum dots coupled with plasmonic spiral antenna

Guanghao Rui,[1, 2, 5] Weibin Chen,[1] Don C. Abeysinghe,[3]
Robert L. Nelson,[4] and Qiwen Zhan[1*]

[1]*Electro-Optics Program, University of Dayton, 300 College Park, Dayton, OH 45469, USA*
[2]*Department of Optics and Optical Engineering, University of Science and Technology of China, Hefei, Anhui 230026, China*
[3]*Department of Electrical and Computer Engineering, University of Cincinnati, Cincinnati, Ohio 45219, USA*
[4]*Air Force Research Laboratory, Wright–Patterson Air Force Base, Dayton, OH 45433, USA*
[5]*ghrui@mail.ustc.edu.cn*
* qzhan1@udayton.edu

Abstract: Coupling nanoscale emitters via optical antennas enables comprehensive control of photon emission in terms of intensity, directivity and polarization. In this work we report highly directional emission of circularly polarized photons from quantum dots coupled to a spiral optical antenna. The structural chirality of the spiral antenna imprints spin state to the emitted photons. Experimental results reveal that a circular polarization extinction ratio of 10 is obtainable. Furthermore, increasing the number of turns of the spiral gives rise to higher antenna gain and directivity, leading to higher field intensity and narrower angular width of emission pattern in the far field. For a five-turn Archimedes' spiral antenna, field intensity increase up to 70-fold simultaneously with antenna directivity of 11.7 dB has been measured in the experiment. The highly directional circularly polarized photon emission from such optically coupled spiral antenna may find important applications in single molecule sensing, quantum optics information processing and integrated photonic circuits as a nanoscale spin photon source.

©2012 Optical Society of America

OCIS codes: (240.6680) Surface plasmons; (350.5610) Radiation; (260.5430) Polarization.

References and links

1. W. L. Stutzman, and G. A. Thiele, Antenna theory and design (Wiley, New York, 1998).
2. T. Kosako, Y. Kadoya, and H. F. Hofmann, "Directional Control of Light by a Nano-Optical Yagi-Uda Antenna," Nature Photon. **4**, 312-315 (2010).
3. P. Mühls chlegel, H. J. Eisler, O. J. F. Martin, B. Hecht, and D. W. Pohl, "Resonant Optical Antennas," Science **308**, 1607-1609 (2005).
4. S. Lal, S. Link, and N. J. Halas, "Nano-Optics from Sensing to Waveguiding," Nat. Photonics **1**, 641-648 (2007).
5. E. Cubukcu, E. A. Kort, K. B. Crozier, and F. Capasso, "Plasmonic Laser Antenna," Appl. Phys. Lett. **89**, 093120 (2006).
6. H. A. Atwater, and A. Polman, "Plasmonics for Improved Photovoltaic Devices," Nat. Mater. **9**, 205-213 (2010).
7. J. A. Schuller, E. S. Barnard, W. Cai, Y. C. Jun, J. S. White, and M. L. Brongersma, "Plasmonics for Extreme Light Concentration and Manipulation," Nat. Mater. **9**, 193-204 (2010).
8. Y. Fu, and J. R. Lakowicz, "Modification of Single Molecule Fluorescence near Metallic Nanostructure," Laser Photonics Rev. **3**, 221-232 (2009).
9. H. Aouani, O. Mahboub, N. Bonod, E. Devaux, E. Popov, H. Rigneault, T. W. Ebbesen, and J. Wenger, "Bright Unidirectional Fluorescence Emission of Molecules in a Nanoaperture with Plasmonic Corrugations," Nano Lett. **11**, 637-644 (2011).
10. A. G. Curto, G. Volpe, T. H. Taminiau, M. P. Kreuzer, R. Quidant, and N. F. Hulst, "Unidirectional Emission of a Quantum Dot Coupled to a Nanoantenna," Science **329**, 930-932 (2010).

11. H. Aouani, O. Mahboub, E. Devaux, H. Rigneault, T. W. Ebbesen, and J. Wenger, "Plasmonic Antennas for Directional Sorting of Fluorescence Emission," Nano Lett. **11**, 2400-2406 (2011).
12. T. Ming, L. Zhao, H. Chen, K. C. Woo, J. Wang, and H. Lin, "Experimental Evidence of Plasmophores: Plasmon-Directed Polarized Emission from Gold Nanorod-Fluorophore Hybrid Nanostructures," Nano Lett. **11**, 2296-2303 (2011).
13. G. Rui, R. L. Nelson, and Q. Zhan, "Circularly Polarized Unidirectional Emission via a Coupled Plasmonic Spiral Antenna," Opt. Lett. **36**, 4533-4535 (2011).
14. Q. Zhan, "Cylindrical Vector Beams: from Mathematical Concepts to Applications," Adv. Opt. Photon. **1**, 1-57 (2009).
15. W. Chen, and Q. Zhan, "Realization of an Evanescent Bessel Beam via Surface Plasmon Interference Excited by a Radially Polarized Beam," Opt. Lett. **34**, 722-724 (2009).
16. R. M. Osgood, N. C. Panoiu, J. I. Dadap, X. Liu, X. Chen, I. Hsieh, E. Dulkeith, W. M. J. Green, and Y. A. Vlasov, "Engineering Nonlinearities in Nanoscale Optical Systems: Physics and Applications in Dispersion-Engineered Silicon Nanophotonic Wires," Adv. Opt. Photon. **1**, 162-235 (2009).
17. R. F. Qulton, V. J. Sorger, T. Zentgraf, R. Ma, C. Gladden, L. Dai, G. Bartal, and X. Zhang, "Plasmon Lasers at Deep Subwavelength Scale," Nature **461**, 629-632 (2009).
18. S. Wang, S. Ota, B. Guo, J. Ryu, C. Rhodes, Y. Xiong, S. Kalim, L. Zeng, Y. Chen, M. A. Teitell, and X. Zhang, Nano Lett. **11**, 3431-3434 (2011).

1. Introduction

Antennas are devices that convert electromagnetic radiation into localized energy, and vice versa [1]. Although antennas are widespread in the radio frequency and microwave regimes, typical optical components rely on geometric optical effects arising from the manipulation of wavefronts with lenses and mirrors. Consequently, optical fields are difficult to be localized within dimensions much smaller than the optical wavelength due to diffraction. In order to get highly confined spot beyond the diffraction limit, nanoscale optical antenna can be used to interface with the far field optical radiation. With the development of modern nanofabrication techniques, the fabrication of optical antenna with sophisticated subwavelength structure becomes possible. Despite the differences between the classical antenna and the emerging optical antenna, they share the equivalent objective and the basic principles of classical antenna design can still be applied in the optical regime [2]. In the past decade, optical antenna has been mostly studied for its function as a receiver, in which case the incident electromagnetic wave's energy shall be efficiently captured by the optical antenna at a certain resonance condition, resulting in strongly enhanced local electromagnetic fields due to surface plasmon polaritons (SPP), oscillations of free electrons in metals that couple to the incident light field. A wide range of applications have arisen for receiving antenna, for instance in sensing, subwavelength and nonlinear optics, nanoscale imaging and spectroscopy and photovoltaics [3-6], exploiting the strong local fields and large absorption cross sections they provide.

Besides functioning as receivers for strong local field generation, optical antennas also offer the capability of tailoring the properties of photons emitted from nanoscale emitters in terms of the emission intensity, directivity and polarization. As reciprocal to a receiver, the transmitting antenna is designed to efficiently convert localized energy to free space propagating optical radiation. By controlling the optical resonances in the vicinity of the emitter, properties of the photon emissions can be modified and controlled. The study for transmitting antenna has been largely boosted by the need of those applications that require high angular sensitivity, such as light-emitting devices, molecular sensing, and unidirectional fluorescent molecular sources [7-9]. Highly directional far-field emission of a linearly polarized beam has been demonstrated experimentally from an array of optical Yagi-Uda antenna [2, 10]. Recently, a nanoaperture surrounded by five concentric circular corrugations has been demonstrated for significant enhancement of the fluorescence count rates per molecule and high emission directivity [9]. Through tuning the groove-nanoaperture distance, the fluorescence directivity can be controlled resulting from the interference phenomenon [11].

2

Features such as enhanced intensity and high directivity of photon emission with the use of optical antenna have been pursued. However, the polarization state aspect of photon emission from optical antennas has received little attention until recently [12, 13]. In traditional antenna engineering, it is well known that right-hand or left-hand circular (RHC and LHC) polarization radiation can be generated from spiral antenna with different handedness [1]. This points out a potential way of using plasmonic spiral antenna to control the emission properties, such as the polarization and emission direction of quantum systems [12]. The goal of this work is to demonstrate the beaming of bright circularly polarized emission from quantum dots coupled with a plasmonic spiral antenna. The beaming of circularly polarized photons requires longitudinal excitation of the quantum dots, which is satisfied with the use a radially polarization illumination. The influences of the parameters of the spiral antenna such as the number of turns and the polarization state of the illumination are also investigated.

2. Methods

2.1 Design of optical spiral antenna and fabrication

The optical antenna structure we proposed in this work is an Archimedes' spiral illustrated in Fig. 1(a). A 150 nm gold film was deposited onto a glass substrate (n = 1.5) by e-beam evaporation. This thickness was chosen to prevent far field direct transmission of the laser through the gold film. Right handed Archimedes' spiral slot with single turn, 2-turn, 3-turn, 4-turn, and 5-turn were fabricated with focused ion beam (FIB) milling (FEI dual beam SEM-FIB NOVA 200 Nanolab system). The FIB was used with an acceleration voltage of 30 kV and a very small ion current of 28 pA to obtain the smallest possible beam diameter (21 nm), thus to guarantee minimal redeposition of Ga in the cut regions and highly vertical sidewalls. In the cylindrical coordinates, the right-handed spiral structure can be descripted as

$$r = r_0 + \frac{\Lambda}{2\pi}\varphi, \tag{1}$$

where Λ equals the surface plasmon polaritons (SPP) wavelength λ_{spp} for a planar gold/air interface. The SPP wavelength λ_{spp} was calculated to be 598.8 nm with 633 nm optical excitation. The groove width is 200 nm and the r_0 equals to $2\lambda_{spp}$. The SEM images of the fabricated sample of right-handed spiral (RHS) structure with 1-5 turns are shown in the insets of Fig. 2(b)-2(f), respectively.

2.2 FEM simulation and physical mechanisms

A full three-dimensional finite element method model (COMSOL) has been developed to numerically investigate the characteristics of the optical spiral antenna. An electric dipole that is placed 5 nm over the center of the spiral surface is used to represent a nanoscale emitter. Numerical modeling indicates that the distance between the electric dipole and the spiral surface does not have significant influence on the emission directivity and polarization except for reducing the emission intensity in the far field as the distance increases. The emission wavelength is set to be 633 nm and the electric current dipole moment equals to 1 m·A. The electric dipole oscillates along z-axis (normal to the spiral surface). The orientation of the oscillation is critical to achieve circularly polarized photon emission in the far field, thus the excitation condition of the emitter needs to be dealt with carefully. With this longitudinally excited dipole, the optical field emitted from this dipole illuminates the spiral structure with the local electric field TM polarized to the spiral slit. The sharp edge of the spiral slit couples light into SPP and reradiate into the far field on the other side of the electric dipole. Through adjusting the parameters of the optical antenna design, the far field emission properties can be tailored.

3

2.3 Experimental setup

In the experiment, quantum dots are adopted as the nano-emitters. As described above, the orientation of the dipole oscillation needs to be normal to the spiral antenna surface in order to obtain circularly polarized photon emission in the far field. According to the simulation, the electric dipole oscillating in the *x-y* plane leads to a split in the center of the far field emission pattern and the emission polarization will be linear. Therefore, to obtain beaming of circularly polarized photon emission from the fluorescent quantum dots, the excitation field needs to be aligned in the longitudinal direction (normal to the surface). Furthermore, illumination with small spot of focus is necessary. The larger the spot size is, the more quantum dots away from the center of the spiral are excited, which give rise to broader emission angular width and strong background noise. These requirements can be fulfilled with a radially polarized excitation source due to its tighter focus and strong longitudinal component [14]. The diagram of the experimental setup is illustrated in Fig. 1(b). A radially polarized beam is generated through coupling laser beam into a few-mode optical fiber [15]. The optical fiber acts as a spatial filter and a polarization mode selector. The optical excitation wavelength is chosen to be 532 nm. Fluorescent Qdots (R) 625 ITK carboxyl quantum dots from Invitrogen were used as the emitters due to its excellent stability and lifetime. The peak emission wavelength (λ_{em} = 625 nm) is slightly smaller than that of designed. However, this affects the results very little. The quantum dots were diluted in isopropyl alcohol with volume ratio 1:10. A small droplet of the diluted quantum dots solution being used as the emitters is dripped on the surface of RHS structure and dried in air. The radially polarized beam coming out of the end of a few-mode fiber is tightly focused onto the gold-air interface of the spiral by an objective lens (Mitutoyo M Plan Apo NIR HR 50 × /0.65) with an NA of 0.65. Under this NA, the peak of longitudinal components at the center of the focal spot is as strong as the peak value of the surrounding transverse component according to numerical calculation. As we will show in the discussions part, the excitation efficiency of longitudinal component is about 12 times higher than the transverse components. Thus, the far field emission is dominated by the longitudinal excitation under the NA we use.
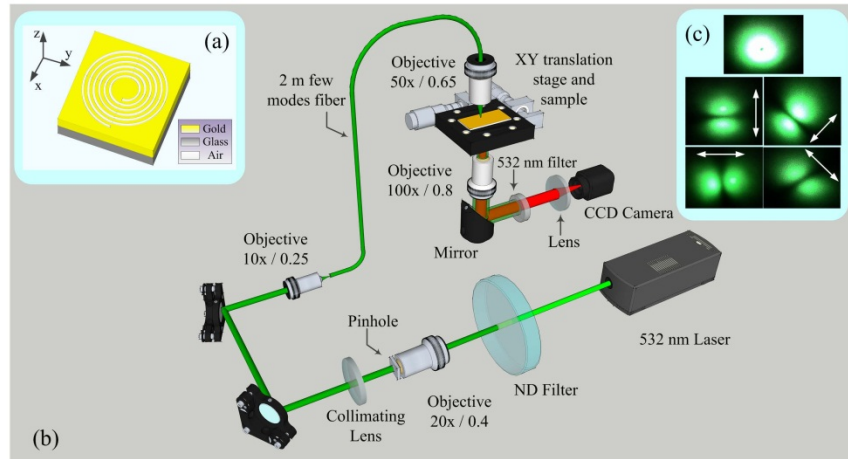

Figure 1. Plasmonic spiral antenna for the control of the photon emission from quantum dots in solution. (a) Diagram of the proposed spiral antenna structure. (b) Experimental configuration. (c) Radially polarized beam pattern generated at the end of the fiber, and pictures of the beam after it passes through a linear analyzer oriented at different angles shown by the arrows.

Through carefully adjusting the *x-y* translation stage, the center of the spiral and the focused radially polarized beam can be aligned. To control the position of the sample precisely, a CCD camera (not shown in setup) is used to capture the images reflecting from

4

the gold-air interface of the spiral. Another inverted objective lens (Nikon LU Plan 100 × /0.8) with an NA of 0.8 below the *x-y* translation stage is used to collect the radiated emission from the glass side. The focal plane of this collecting objective lens is adjusted to the glass-air interface of the sample. A 532 nm notch filter after the inverted objective lens filters out the excitation wavelength. After being slightly focused by a lens, the red fluorescence signals are collected by another CCD camera. Fig. 1 shows the doughnut pattern of the generated radially polarized beam. Pictures of the beam after it passes through a linear polarizer oriented at different angles are also captured to confirm the radial polarization distribution. The radially polarized beam is strongly focused to excite the quantum dots near the center of the spiral and the fluorescence signals on the other side of the spiral antenna are collected by the CCD camera.

3. Experimental results and discussion

The collected fluorescence signals are shown in Fig. 2(a)-2(f). For a glass substrate without spiral structure, the image contains a single disk with its radius representing the maximum collection angle of the inverted objective at 53° (shown in Fig. 2(a)). While for all the other samples with RHS structures, the image contains an additional bright spot centered on the optical axis. The illumination and the position of collecting objective lens are kept unchanged during the experiment so the results for spiral with different number of turns are comparable. The line-scans of the simulated and experimental fluorescence emission patterns along *x* and *y* axes are shown in Fig. 3(a)(b) and Fig. 3(c)(d) respectively. By adding more turns of the spiral, the full-width-half-maximal (FWHM) of the emission pattern in the far field can be further reduced. The fluorescence emission intensity can also be further improved because of larger receiving area for SPP generation and reradiation. Please note that the intensities in Fig. 2 (a)-(d) have been multiplied by a factor to show the figures clearly.
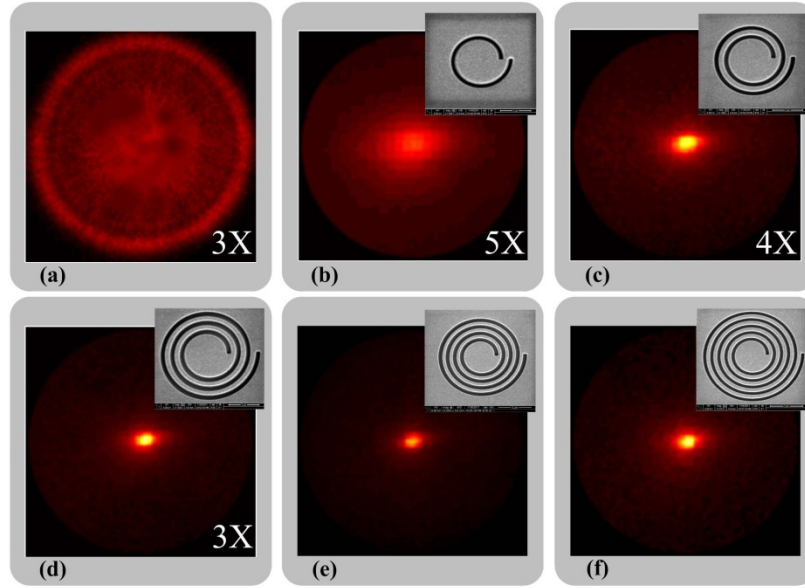

Figure 2. Fluorescence intensity distributions in the back focal plane of a 0.8 NA objective lens. (a) Emission pattern for the case of no spiral structure. Please note that the intensity of this image has been magnified by a factor of five to show the field distribution clearly. (b)-(f), Emission patterns for a RHS structure with an increasing number of turns from 1 to 5. SEM pictures of the spiral antennas are shown as the insets. The intensities in (a), (b), (c) and (d) are multiplied by a factor to ease viewing the figures.

5

Overall the experimental data agree well with the simulation. Higher fluorescence intensity and narrower angular width of the emission patterns can be clearly seen for optical spiral antenna with more turns, although the FWHMs are slightly broader in the experiment. The differences are mainly caused by different number of quantum dots being excited. In the COMSOL model, only one electric dipole is used to excite the RHS structure. But in the experiment, although the solution of quantum dots has already been diluted, the excitation of single quantum dot still cannot be achieved. A bunch of quantum dots near the center of the spiral are excited, leading to the larger angular width of the emission pattern. For spiral antenna with 5 turns, the emission pattern is highly directional, with FWHM of $10°$ and $11°$ along the x-direction and y-direction respectively. The fluorescence peak intensity is increased up to 70 fold compared to the average intensity of the case of no spiral structure, which is higher than that of spiral antenna with fewer turns. To quantify the collimation in the direction normal to the surface, the antenna directivity defined as $D = 10 \log_{10} (2\pi I_{peak}/I_{average})$, where I_{peak} is the far-field peak intensity and $I_{average}$ is the average field integrated over the lower half-space for the case of no spiral antenna, is calculated to be 11.4 dB for the 5-turn spiral antenna.
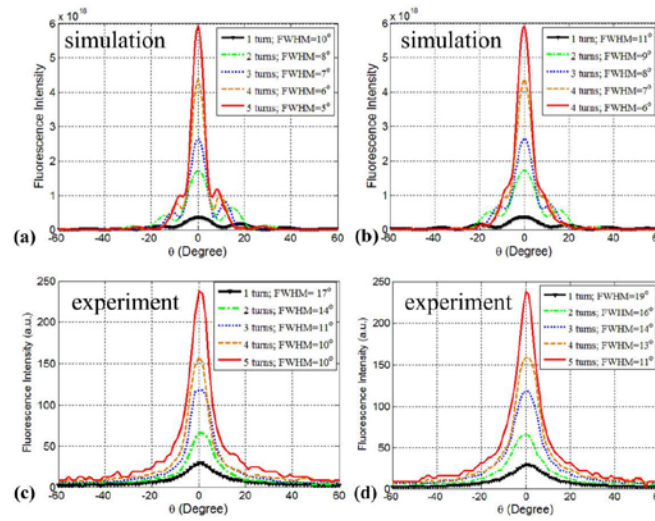
Figure 3. Line-scans through the center of the emission patterns in the far field along x- and y-axes. Line-scans in the (a, c) x-z plane and (b, d) y-z plane from simulation and experimental results respectively.

6

The fluorescence emission carries polarization property essentially determined by the handedness of the spiral. The polarization state of the radiated emission should be LHC for the RHS structure [13]. To verify this feature, a circular analyzer composed of a quarter-wave plate followed by a linear polarizer is placed behind the collection objective lens. The angle between fast axis of quarter-wave plate and polarization direction of linear polarizer is set to 45°. The emission pattern after the circular analyzer is shown in Fig. 4. For the LHC polarizer, there is a dark hole in the center of the radiation pattern (shown in the inset of Fig. 4(b)), while a central peak could be observed when the emitted beam go through a RHC polarizer (shown in the inset of Fig. 4(a)), which is a manifestation of RHC polarization for the fluorescence emission. Circular polarization extinction ratio is defined as I_1/I_2, where I_1 and I_2 are the fluorescence intensities in the center of the emission pattern after insertion of left and right circular polarizer respectively. A peak extinction ratio near 10 has been achieved in the center for RHS structure with 5-turn spiral antenna. A linescan of circular polarization extinction ratio is shown in Fig. 4 (c). The main lobe of the emission in the far field still holds the RHC polarization.
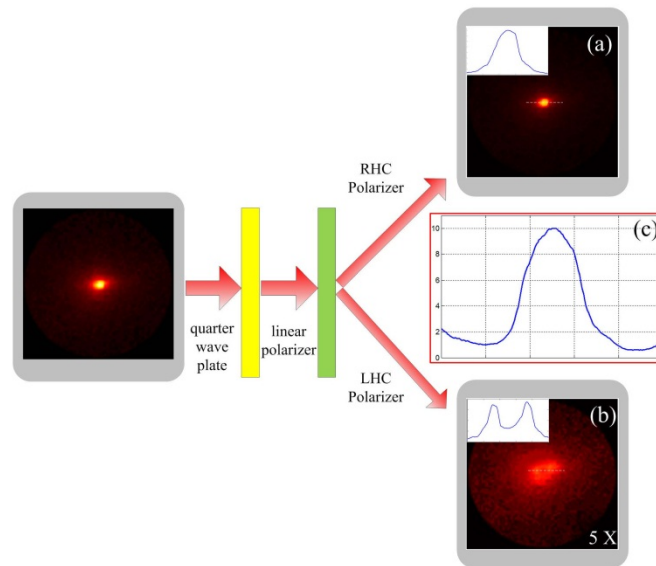

Figure 4. Method for measuring the circular polarization extinction ratio of the emission. The right pictures show the radiated emissions filtering by (a) a RHC polarizer and (b) a LHC polarizer that is composed of a quarter-wave plate and a linear polarizer. The insets show the linescan through the center. Please note that the intensity in (b) has been multiplied by a factor of 5 in order to obtain a clear image. (c) Linescan of circular polarization extinction ratio.

Other than the longitudinal excitation with radially polarized illumination, the effect of linearly polarized illumination is also investigated both numerically and experimentally. Linearly polarized Gaussian beam was generated with the same few mode fiber through careful alignment (shown in Fig. 5(a)). The power of the Gaussian beam is adjusted to the same level of radially polarized beam used above. Then the Gaussian beam is focused onto the center of the 5-turn spiral antenna with the same collection optics. The simulated and measured emission patterns are shown in Fig. 5(b) and 5(c) respectively. As expected, a split spot with a dark center is observed, which is caused by the destructive interference of SPP at azimuthal directions. It is worthy of noting that the fluorescence intensity of radiated emission for linearly polarized illumination is much lower than that from radially polarized illumination, the maximal fluorescence intensity of radiated emission for radially polarized illumination is nearly 12 times larger than that from linear polarization. This is consistent with our simulation results that the coupling efficiency of the longitudinal field component is much

7

higher than the in-plane ones. This indicates that the emission features shown above for the longitudinally excited fluorescent emitter can still be largely maintained even for a bunch of emitters with orientations deviated from the normal direction.
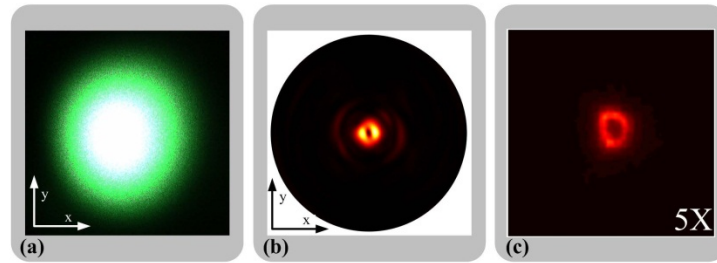

Figure 5. Influence of illumination with transverse polarization. (a) Linearly (x-) polarized Gaussian beam pattern generated at the end of the fiber. (b) Simulated electric field intensity distribution in the far field. (c) Emission patterns from experimental results. The intensity has been multiplied by a factor of 5 in order to obtain a clear image.

4. Conclusions

In conclusion, the feasibility of beaming circularly polarized photons emitted from quantum dots coupled to a plasmonic spiral lens has been demonstrated experimentally. With increasing number of turns of the spiral antenna, the emission brightness becomes higher and FWHM of the angular emission pattern in the far field can be reduced further. The emitted photons from this spiral antenna coupled emitter carry the spin essentially determined by the chirality of the spiral optical antenna. Imprinting the spin state to the emitted photons requires longitudinally oriented field from the emitter, which is realized with radially polarized excitation in the experiment. However, such longitudinal feeding can be realized with highly confined nanoscale modes from nanowire waveguide [16] or nano laser [17], paving the way towards a fully integrated nanodevices. The nanoscale spin photon source demonstrated in this work is believed to have high relevance for the applications in sensing, which could further improve the signal to noise ratio of a sensing technique reported recently in [18], it also may find many potential applications in quantum optical information processing and integrated photonic circuits.

Acknowledgements

Approved for public release; distribution unlimited.

LIST OF ACRONYMS, ABBREVIATIONS, AND SYMBOLS

Acronym	Definition
SPP	Surface Plasmon Polaritons
RHC	Right-Hand Circular
LHC	Left-Hand Circular
FIB	Focused Ion Beam
RHS	Right-Handed Spiral
CCD	Charge-Coupled Detector
FWHM	Full Width at Half Maximum